Distribution Agreement

In presenting this thesis as a partial fulfillment of the requirements for a degree from Emory University, I hereby grant to Emory University and its agents the non-exclusive license to archive, make accessible, and display my thesis in whole or in part in all forms of media, now or hereafter now, including display on the World Wide Web. I understand that I may select some access restrictions as part of the online submission of this thesis. I retain all ownership rights to the copyright of the thesis. I also retain the right to use in future works (such as articles or books) all or part of this thesis.

Selin Ekici April 14, 2020

Immunometabolic profiles in glioma studied with ^{1}H HRMAS NMR

By

Selin Ekici

Candace C. Fleischer, Ph.D.
Adviser

Department of Chemistry

Candace C. Fleischer, Ph.D.

Committee Member

Jeremy Weaver, Ph.D.

Committee Member

Michael McCormick, Ph.D.

Committee Member

2020

Immunometabolic profiles in glioma studied with ^{1}H HRMAS NMR

By

Selin Ekici

Candace C. Fleischer, Ph.D.

Adviser

An abstract of
a thesis submitted to the Faculty of Emory College of Arts and Sciences
of Emory University in partial fulfillment
of the requirements of the degree of
Bachelor of Science with Honors

Department of Chemistry

2020

Abstract

Immunometabolic profiles in glioma studied with ^{1}H HRMAS NMR

By Selin Ekici

Gliomas are one of the most common types of brain tumors, with 20,000 cases diagnosed every year in the United States alone. Developing specific imaging biomarkers may aid in noninvasively diagnosing and monitoring treatment response in order to improve the prognosis of gliomas. A common property of cancer is the Warburg effect, in which cancer cells use aerobic glycolysis over oxidative phosphorylation, enabling glycolytic byproducts to serve as the precursors for the synthetic biomass needed for cancer proliferation. The precursors for the synthetic biomass arise from glutamine metabolism, which provides nitrogen for the biomass that supports the Warburg effect and enables rapid cancer growth. Moreover, inflammation in the tumor microenvironment increases the expression of enzymes that metabolize glutamine. As glutamine is one of the main substrates for cellular growth in gliomas, it may be a potential imaging biomarker for prognosis and treatment monitoring. The goal of this study was to investigate the relationship between glutamine and inflammation in the tumor microenvironment. ^{1}H high-resolution magic angle spinning (HRMAS) nuclear magnetic resonance (NMR) spectra were acquired from 16 histologically-confirmed ex vivo human glioma samples (World Health Organization grade II=5; grade III=6; grade IV=5) and metabolites were quantified using LCModel. Concentrations of interleukin (IL)-1A, IL-1B, IL-8, IL-6, tumor necrosis factor-α (TNF-α), and C-reactive protein (CRP) in glioma samples were quantified using electrochemiluminescence assays. Principal component analysis (PCA) was performed to limit multiple comparisons of the inflammatory markers. Glutamine, glutamate, glutathione, lactate, and alanine increased significantly with tumor grade ($p \leq .05$). Concentrations of inflammatory markers IL-1A, IL-1B, IL-6, and IL-8 also increased with tumor grade ($p \leq .05$). Glutamine, alanine, glutathione, and lactate were positively associated with the first inflammatory marker PC, and myo-inositol was positively associated with the second PC. Our findings indicate that inflammation is associated with metabolic reprogramming and identifies glutamine as a potential biomarker for metabolic reprogramming in gliomas. Future work will translate the investigation of glutamine as an imaging biomarker to in vivo studies.

Immunometabolic profiles in glioma studied with ^{1}H HRMAS NMR

By

Selin Ekici

Candace C. Fleischer, Ph.D.

Adviser

A thesis submitted to the Faculty of Emory College of Arts and Sciences
of Emory University in partial fulfillment
of the requirements of the degree of
Bachelor of Science with Honors

Department of Chemistry

2020

Acknowledgments

Firstly, I would like to thank my advisor, Dr. Candace Fleischer for the continuous support of the research for this Honor's thesis. Since I joined her lab, she has been a mentor for my research, my career, and my personal life. Dr. Fleischer shows by example what it means to work hard for your goals and has helped me grow both as a scientist and a person.

I would also like to thank my other committee members, Dr. Weaver and Dr. McCormick. Their support of my work and understanding during these challenging times has made the completion of this Honor's thesis possible.

I also want to thank the other members in the Fleischer lab. This research would not be possible without Maame, Dong-Suk, and Kelly's feedback on presentations as well as their ongoing support.

Last but not the least, I would like to thank my friends and family for supporting my goals, and for their unending words of encouragement throughout my college career.

Table of Contents

Figures

Tables

1. Introduction

Gliomas are one of the most common classes of brain tumors, with grade IV glioblastomas (GBM) comprising 80% of malignant tumors.[1-3] Gliomas are highly heterogeneous tumors comprised of cells with multiple genetic and phenotypic signatures, and this heterogeneity may contribute to the high rates of treatment resistance.[2, 3] Moreover, gliomas infiltrate deep into brain tissue. Complete surgical resection is challenging, leading to high recurrence rates.[4] Current clinical practice for high grade gliomas includes maximal safe resection and a combination of chemotherapy and radiation therapy, but due to their heterogeneity, infiltrative nature, and treatment resistance, gliomas have a poor prognosis.[2, 5] Imaging biomarkers may provide a noninvasive method of diagnosing and monitoring response to treatment. Developing noninvasive and specific biomarkers may ultimately improve the prognosis of gliomas.

A hallmark of many cancers is metabolic reprogramming. The most well-known example is the Warburg effect, where carcinogenic cells reprogram their metabolism to rely on aerobic glycolysis over more energy-efficient mitochondrial oxidative phosphorylation.[6-8] Metabolic reprogramming induces high glycolytic flux that maintains the ATP reservoir needed for cancer cells to survive, but more importantly provides precursors for the nucleotides, amino acids, and lipids needed to proliferate.[7] The demand for carbon, nitrogen, and reducing agents are so high that up to 90% of the glucose in tumor cells is converted to lactate and alanine, both downstream glycolytic byproducts used for producing fatty acids and NADPH.[7-11] However, glucose alone cannot provide the nitrogen-based compounds and sufficient TCA cycle intermediates required for cancer cell proliferation.

There is evidence to suggest that this demand is met with glutamine, an amino acid that serves as a precursor for the neurotransmitters glutamate and γ-aminobutyric acid (GABA).[12, 13] Glutaminolysis, or glutamine catabolism, fills several crucial roles in brain cancer. As one of the most abundant amino acids in the brain, glutamine is readily available for breakdown in cells and maintains high metabolic flux by supplying intermediates to the TCA cycle. Its products include lactate, glutamate, and alanine, which are used to generate NADPH, fatty acids, amino acids, and nucleotides.[9, 14, 15] Glutamine is not only used for energetics and division, it can also break down to the antioxidant glutathione (GSH) and upregulate the pentose phosphate pathway (PPP), which allow cells to evade attack from reactive oxygen species that would otherwise kill healthy cells. The increase in GSH and PPP products have been linked to the high rates of treatment resistance in gliomas, primarily due to the increased ability to neutralize free radicals and reduce stress response.[11, 14] Cancer cells can develop a glutamine dependence due to its importance for proliferation, and pharmacologic strategies are increasingly targeting glutamine pathways as a promising avenue for new treatments.[10, 15-17]

Glutamine metabolism is also heavily influenced by inflammation, which is often present in the tumor microenvironment due to oncogene activation and constitutive inflammatory cytokine production by tumor cells.[8, 18] Inflammation is an early indicator of tumor progression, and chronic inflammation contributes to proliferation and metastasis by inducing immunosuppression and extracellular matrix remodeling.[19, 20] Inflammatory cells further aggravate metabolic dysregulation by releasing growth factors that activate NF-kB and STAT3, which promote the release of glutamine into the tumor microenvironment and upregulate the expression of enzymes involved in glutaminolysis.[20-24] While glutamine and glutaminolysis are increasingly common pharmacologic targets, glutamine as an imaging biomarker is largely

unexplored. Given the central role of glutamine in providing energy for cancer cells, and the recent increase in treatment strategies that target the glutamine pathway, we hypothesize that glutamine may be a potential imaging biomarker for prognosis, stratification, and treatment monitoring.

Multi-modal studies that employ metabolomics complemented by immunoassays can identify tumor metabolites and inflammatory markers that are indicative of the crosstalk between inflammation and glutamine metabolism. Nuclear magnetic resonance (NMR) techniques can quantify metabolite concentrations within ex vivo glioma tissue, and advancements in high-resolution magic angle spinning (HRMAS) NMR have improved the sensitivity of the technique.[25-27]

NMR and its in vivo analog, magnetic resonance spectroscopy (MRS),[28] have been used extensively to identify metabolic biomarkers for differentiating between glioma subtypes, grading, and characterizing response to treatment.[29-32] However, NMR-based techniques provide snapshots of metabolic information, without the context of inflammatory drivers and mediators. Multi-modal studies that combine NMR metabolomics with immunoassays may better capture the interplay between tumor metabolism and the inflammatory microenvironment. An ex vivo approach was used to characterize immunometabolic profiles in the glioma microenvironment and identify new candidates for biomarker development. ^{1}H HRMAS NMR revealed an upregulation of glioma metabolites associated with glutaminolysis including glutamate, lactate, and alanine, and these metabolites were significantly correlated with pro-inflammatory cytokines. This multi-modal approach lays the groundwork for more comprehensive profiling of glutamine metabolism in gliomas, motivating future studies using MRS to non-invasively quantify glutamine in vivo.

2. Methods

2.1 Human Glioma Tissue Samples

Sixteen histologically-confirmed glioma samples (World Health Organization (WHO) grade II=5; grade III=6; grade IV=5) collected during surgical resection or excision from human brain tumor patients were obtained from the Cancer Tissue and Pathology Biobank (Emory Winship Cancer Institute). Patient inclusion criteria included samples containing >40% tumor and a diagnosis of diffuse astrocytoma, infiltrating astrocytoma, oligodendroglioma, anaplastic oligodendroglioma, anaplastic astrocytoma, glioblastoma, high grade astrocytoma, or high grade glioma. Patients <18 years old were excluded. Samples from eight males and eight females were included. The age range for all patients was 28-71 years old with mean age ± standard deviation (SD) = 45 ± 13 years. Ten samples were from patients that were isocitrate dehydrogenase (IDH)-1 positive and one was IDH-2 positive (Table 1).[33-35] Tissue samples were flash frozen immediately after surgery and stored at -80 °C prior to batch analysis.

Table 1. Glioma tissue sample characteristics

Specimen	Sex[a]	Race[b]	Age at Collection	Histologically Confirmed Diagnosis	WHO grade	IDH Status[c]
1	M	C	36	Anaplastic Oligodendroglioma	III	IDH-1 mut
2	F	AA	28	Anaplastic Oligodendroglioma	III	IDH-2 mut
3	F	C	54	Oligodendroglioma	II	IDH-1 mut
4	F	C	50	Glioblastoma	IV	WT
5	F	C	45	Oligodendroglioma	II	IDH-1 mut
6	F	C	38	Anaplastic Astrocytoma with Gemistocytic Features	III	IDH-1 mut
7	M	C	62	Glioblastoma	IV	WT
8	M	C	70	Glioblastoma	IV	WT
9	M	C	38	Anaplastic Astrocytoma	III	IDH-1 mut
10	F	C	35	Oligodendroglioma	II	IDH-1 mut
11	M	AA	33	Diffuse Astrocytoma	II	IDH-1 mut
12	F	C	36	Anaplastic Oligodendroglioma	III	IDH-1 mut
13	M	AA	45	Oligodendroglioma	II	IDH-1 mut
14	M	AA	41	Residual Glioblastoma with Therapy-Related Changes	IV	IDH-1 mut
15	M	C	71	Glioblastoma	IV	WT
16	F	C	50	Anaplastic Astrocytoma	III	WT

[a]M=Male; F=Female

[b]C=Caucasian; AA=African American

[c]IDH-1mut=IDH-1 mutated; IDH-2 mut=IDH-2 mutated; WT=Wild type

2.2 Electrochemiluminescence Assays

Immunoassays were performed on tissue (≥10 mg) that was homogenized in 1x homogenization buffer (125 mM Tris, 15 mM $MgCl_2$, and 2.5 mM EDTA) with 1% Triton X-100 and protease inhibitor (Roche). Total protein was quantified with a bicinchoninic acid (BCA) assay. Inflammatory markers were quantified in duplicate from tissue lysate using electrochemiluminescence assays according to manufacturer's instructions (Meso Scale Diagnostics, U-Plex Biomarker Assay, K156067l-1; V-Plex Human CRP Kit, K151STD-1). Concentrations were obtained for interleukin (IL)-1A, IL-1B, IL-8, IL-6, IL-10, IL-17A, interferon (IFN)-γ, tumor necrosis factor (TNF)-α, and C-reactive protein (CRP). Limits of detection for each inflammatory marker are shown in Table 2.

Table 2. Limits of detection of inflammatory markers

Inflammatory Marker	Detection Limit (pg/mL)
CRP	1.33
IFN-γ	1.7
IL-1A	0.98
IL-1B	0.15
IL-6	0.44
IL-8	0.15
IL-10	0.14
IL-17A	2.6
TNF-α	0.54

2.3 HRMAS NMR Spectroscopy

To prepare samples for solid state HRMAS NMR, frozen tissue (10-15 mg) was aliquoted using a 2 mm biopsy punch (Braintree Scientific, Inc, MTP-33-31) and placed in an 80 μL HRMAS disposable insert (Bruker, B4493) inside a 4 mm zirconium oxide HRMAS rotor (Bruker, H14355). All NMR experiments were performed at 4 °C using a 600 MHz NMR spectrometer with an HRMAS probe (Bruker, AVANCE III). NMR spectra were acquired using both free induction decay (FID) and Carr-Purcell-Meiboom-Gill (CPMG) pulse sequences with a pre-saturation water suppression pulse and the following parameters: MAS spinning speed=4000 Hz; complex data points=16,384; spectral bandwidth=8013 Hz; N=512. Brain metabolite concentration ratios and Cramer-Rao lower bounds (CRLBs) were estimated using LCModel[36] with a gamma-simulated 26-metabolite basis set containing MR-detectable metabolites present in gliomas (alanine (Ala), ascorbate (Asc), aspartate (Asp), creatine (Cr), phosphocreatine (PCr), ethanolamine (Eth), GABA, glucose (Glc), glutamine (Gln), glutamate (Glu), glycine (Glyc), glycerophosphocholine (GPC), phosphocholine (PCh), GSH, 2-hydroxyglutarate (2-HG), myo-Inositol (Ins), lactate (Lac), *N*-acetylaspartate (NAA), *N*-acetylaspartylglutamic acid (NAAG), phosphoethanolamine (PE), propylene glycol (PGC), *scyllo*-Inositol (Scyllo), serine (Ser), taurine (Tau), valine (Val), and acetate (Act)).[37]

2.4 Statistical Analysis

Statistical analysis was performed with SPSS (IBM, v26.0). To determine the quality of the LCModel fit to the data, metabolite CRLBs acquired with the FID and CPMG pulse sequences were compared using a paired two sample t-test. All subsequent statistical analyses were performed on concentration ratios obtained from the CPMG pulse sequence for metabolites with CRLBs ≤30. To determine differences in metabolite and inflammatory marker concentrations as a function of grade, non-parametric Kruskal-Wallis tests were performed with

post-hoc pair-wise Dunn's tests. A Bonferroni correction was applied to the test statistic of the Dunn's test to correct for multiple comparisons. One-way analysis of covariance (ANCOVA) was also used to evaluate differences in metabolites and inflammatory markers while accounting for age at diagnosis as a covariate in the analysis.

To limit multiple comparisons for the detected inflammatory markers, principal component analysis (PCA) was used to reduce the dimensions of inflammatory marker concentrations and identify orthogonal principal components (PCs) that encapsulate the maximum amount of variance within the data set.[38] Normality of inflammatory marker concentrations were determined by plotting the distributions in histograms. As inflammatory marker concentrations were not normally distributed, data was log-transformed prior to PCA. PCs with eigenvalues ≥1 were retained. Each PC was comprised of loadings (a value from -1 to 1) from individual inflammatory markers. Inflammatory markers with loading components greater than |0.45| were used to determine the significant contributions to each PC.[39] Associations between NMR-quantified tumor metabolites and inflammatory marker PCs were determined with linear PC regressions. Significance for all analyses was determined using $p \leq .05$.

3. Results

Representative NMR spectra acquired with FID and CPMG sequences are shown in Figure 1.[33, 34] Metabolite CRLBs for Lac and Ins were significantly lower for spectra acquired with CPMG compared to the FID sequence ($p=.049$ and $p=.015$ for Lac and Ins, respectively); Table 3).[33, 34] While there were no statistically significant differences in CRLBs observed for the other metabolites, most metabolites could be quantified with LCModel from spectra acquired with the CPMG pulse sequence, whereas many metabolites acquired with the FID sequence were not detected. For example, Lac was quantifiable from three of the spectra acquired with FID

compared to 12 spectra acquired with CPMG (Table 3). A representative spectrum acquired with the CPMG sequence, along with LCModel fit to the data, is shown in Figure 2.[33, 34]

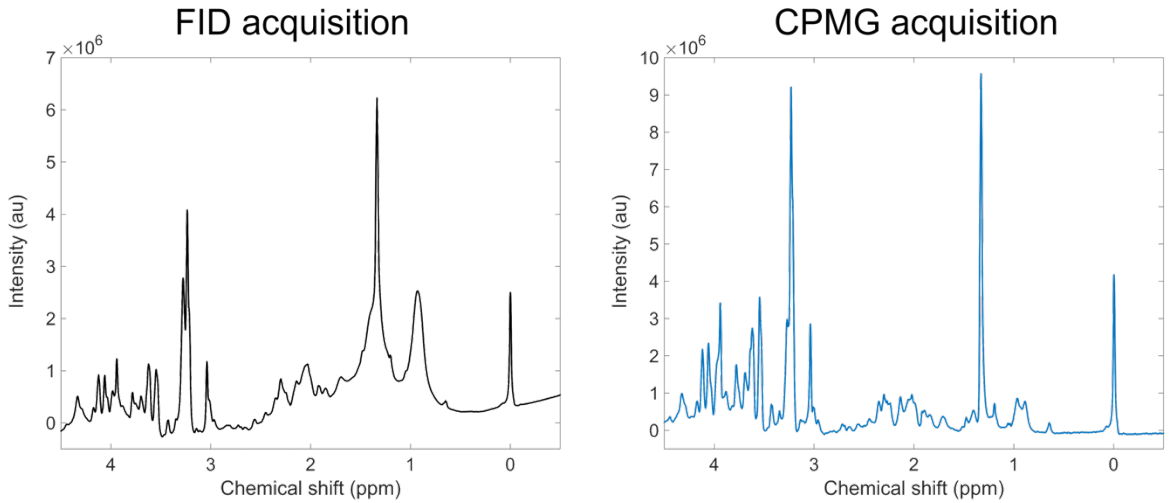

Figure 1. Representative spectra acquired with FID and CPMG sequences

Table 3. Mean metabolite CRLBs for FID and CMPG sequences

Metabolite[a]	FID CRLB[b]	# Spectra with Detected Metabolite	CPMG CRLB[c]	# Spectra with Detected Metabolite	p-value[d]
Gln	8.5	8	15.9	12	.10
Glu	12.3	8	15.3	12	.36
Lac	59.7	3	8.7	12	**.049**
NAA	68.8	8	32.3	11	.18
Ins	12.4	11	8.5	12	**.015**
Cr + PCr	14.0	9	9.1	12	.083
GPC + PCh	26.3	6	20.2	12	.13

[a]Metabolite ratios to Cr + PCr are reported
[b]FID=Free Induction Decay; CRLB=Cramer Rao Lower Bound
[c]CPMG=Carr-Purcell Meiboom Gill
[d]Bolded values indicate statistical significance (p≤.05)

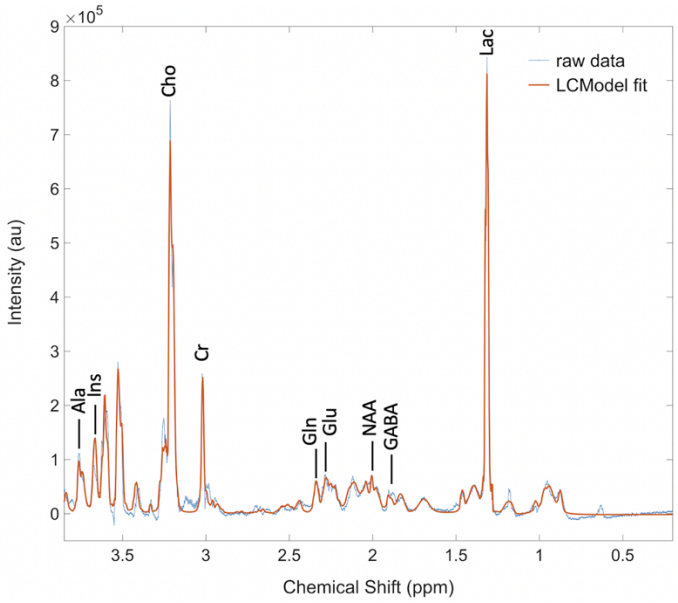

Figure 2. Representative HRMAS spectra of glioma tissue acquired with the CPMG sequence

Several metabolites varied significantly as a function of WHO grade when analyzed with a Kruskal-Wallis H-Test and post-hoc pair-wise Dunn's tests including Ala, Gln, Glu, PCh, GSH, and Lac (Table 4).[35] GPC, GABA, 2-HG, Ins, and NAA+NAAG were not significantly different between WHO grades. Asp could only be quantified in one sample. Importantly, total Cr (Cr + PCr) was used to normalize metabolite concentrations and was not significantly different between groups (Table 4).[35] After controlling for age using an ANCOVA, the log-transformed Ala, Gln, and GSH concentrations were still significantly different across WHO grades (Table 6). Inflammatory markers including IL-1B, IL-6, IL-8, and TNF-α concentrations increased significantly with grade when analyzed with a Kruskal-Wallis H-Test and post-hoc pair-wise Dunn's tests (Table 7, Figure 3), while IL-1A and CRP did not vary significantly ($p>.05$, Table 8).[35] Concentrations of IL-10, IL-17A, and IFN- γ were below the detection limits for all samples (Table 2). After including age at diagnosis as a covariate, log(IL-1B), log(IL-6), and IL-8 concentrations varied significantly with grade (Table 9).

PCA resulted in two inflammatory marker PCs (PC-1 and PC-2). PC-1 contained contributions from four inflammatory markers (IL-1A, IL-1B, IL-8, CRP), and PC-2 contained significant contribution from only CRP (Table 10).[35] Ala, Gln, GSH, and Lac concentration ratios were positively associated with PC-1 (p=.043; p=.067; p<.001; p=.030, respectively) while Ins was positively associated with PC-2 (p=.015) (Table 11, Figure 4).[35] The remaining metabolites were not significantly associated with either of the inflammatory PCs (p>.05).

Table 4. Metabolites as a function of WHO grade evaluated by Kruskal Wallis H-test

Metabolite	H-Test (p-value)[b]
Ala	**.024**
Cr	.40
PCr	.22
GABA	1.00
Gln	**.038**
Glu	**.021**
GPC	.42
PCh	**.039**
GSH	**.012**
2HG	.67
Lac	**.018**
Ins	.59
NAA+NAAG	.13

[a]Metabolite ratios to Cr + PCr are reported
[b]Bolded values indicate statistical significance (p≤.05); refer to Table 5 for post-hoc test
[c]Bonferroni-adjusted p-values

Table 5. Tumor metabolites that varied significantly as a function of WHO grade

Metabolite[a]	H-Test (p-value)[b]	Post-hoc pair-wise comparison (p-values)[c]		
		II vs. III	III vs. IV	II vs. IV
Ala	**.024**	>.99	.13	**.031**
Gln	**.038**	>.99	.073	.10
Glu	**.021**	>.99	**.039**	.055
GSH	**.012**	.90	.13	**.011**
Lac	**.018**	>.99	**.028**	.051

[a]Metabolite ratios to Cr + PCr are reported

[b]Bolded values indicate statistical significance (p≤.05)

[c]Bonferroni-adjusted p-values

Table 6. Tumor metabolites as a function of WHO grade evaluated by ANCOVA F-Test

Metabolite[a]	ANCOVA F-Test (p-value)[b]	Post-hoc pair-wise comparison (p-values)[c]		
		II vs. III	III vs. IV	II vs. IV
Log(Ala)	**<.01**	.53	**.021**	**<.01**
Gln	**.029**	>.90	**.048**	**.037**
GSH	**<.01**	>.90	**<.01**	**<.01**

[a]Metabolite ratios to Cr + PCr are reported

[b]Bolded values indicate statistical significance (p≤.05)

[c]Bonferroni-adjusted p-values

Table 7. Inflammatory marker concentration differences as a function of WHO grade

Inflammatory Markers	H-Test (p-value)[b]	Post-hoc pair-wise comparison (p-values)[c]		
		II vs. III	III vs. IV	II vs. IV
IL-1A	**.044**	>.99	**.035**	**.021**
IL-1B	**.017**	.84	.50	**.013**
IL-6	**.041**	>.99	.14	.14
IL-8	**.015**	>.99	**.030**	**.042**

[a]Inflammatory marker concentrations in pg/μL are reported

[b]Bolded values indicate statistical significance (p≤.05)

[c]Bonferroni-adjusted p-values

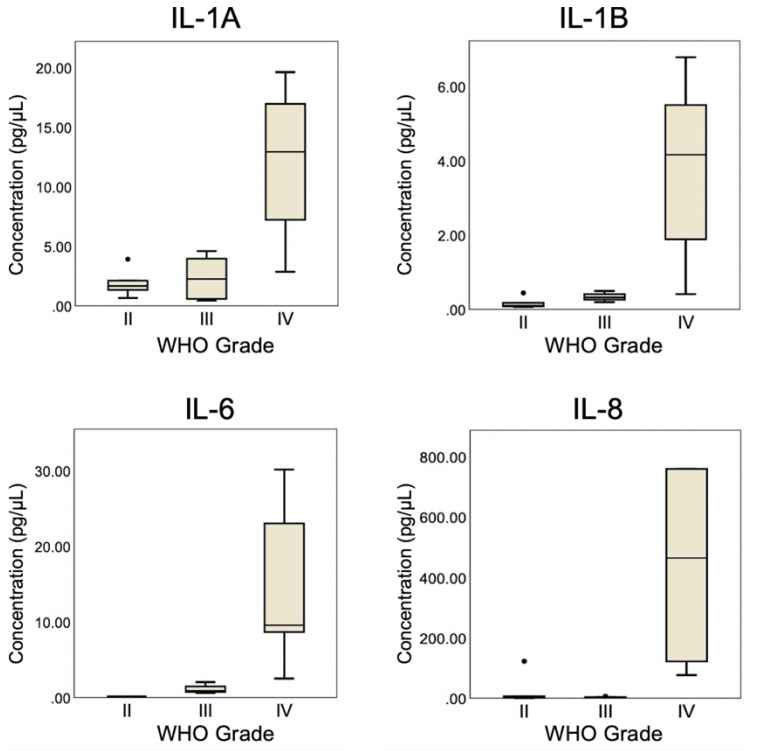

Figure 3. Box plots of inflammatory marker differences as a function of WHO grade

Table 8. Tumor inflammatory markers as a function of WHO grade evaluated by Kruskal Wallis H-Test

Inflammatory Marker	H-Test (p-value)[b]
CRP	.63
IFN- γ	---
IL-1A	**.044**
IL-1B	**.017**
IL-6	**.041**
IL-8	**.015**
IL-10	---
IL-17A	---
TNF- α	---

[a]Inflammatory marker concentrations in pg/µL are reported

[b]Bolded values indicate statistical significance; dashed lines refer to concentrations below the limit of detection; refer to Table 7 for post-hoc tests

[c]Bonferroni-adjusted p-values

Table 9. Tumor inflammatory markers as a function of WHO grade evaluated by ANCOVA F-Test

Inflammatory Marker	ANCOVA F-Test (p-value)[b]	Post-hoc pair-wise comparison (p-values)[c]		
		II vs. III	III vs. IV	II vs. IV
log(IL-1A)	**.042**	>.99	.13	.088
log(IL-1B)	**.002**	.654	**.020**	**.002**
IL-8	**.020**	>.99	**.012**	**.016**

[a]Inflammatory marker concentrations in pg/μL are reported

[b]Bolded values indicate statistical significance ($p \leq .05$)

[c]Bonferroni-adjusted p-values

Table 10. Inflammatory marker loadings onto individual principal components

Inflammatory Marker	Component Loadings	
	PC-1 (62.4% of variance)	PC-2 (27.09% of variance)
IL-1B	0.94	-0.010
IL-8	0.91	-0.22
IL-1A	0.87	-0.27
CRP	0.56	0.82

Table 11. Linear regressions of significant metabolite concentrations and inflammatory principal component scores

Metabolite[a]	PC-1		PC-2	
	β ± SD[b]	p-value[c]	β ± SD	p-value
Ala	0.72±0.12	**.043**	-0.39±0.15	.34
Gln	0.67±0.30	.067	-0.11±0.40	.79
Glu	0.52±0.37	.15	-0.20±0.43	.60
GPC + PCh	0.38±.10	.31	.37±0.09	.33
GSH	0.96±0.04	**<.001**	-.008±0.13	.98
Lac	0.68±1.38	**.030**	-0.30±1.7	.40
Ins	0.22±0.29	.55	0.74±0.19	**.015**
NAA + NAAG	0.68±1.38	.73	-0.40±0.17	.37

[a]Metabolite ratio to Cr + PCr

[b]Standardized coefficients

[c]Bolded values indicate statistical significance (p≤.05)

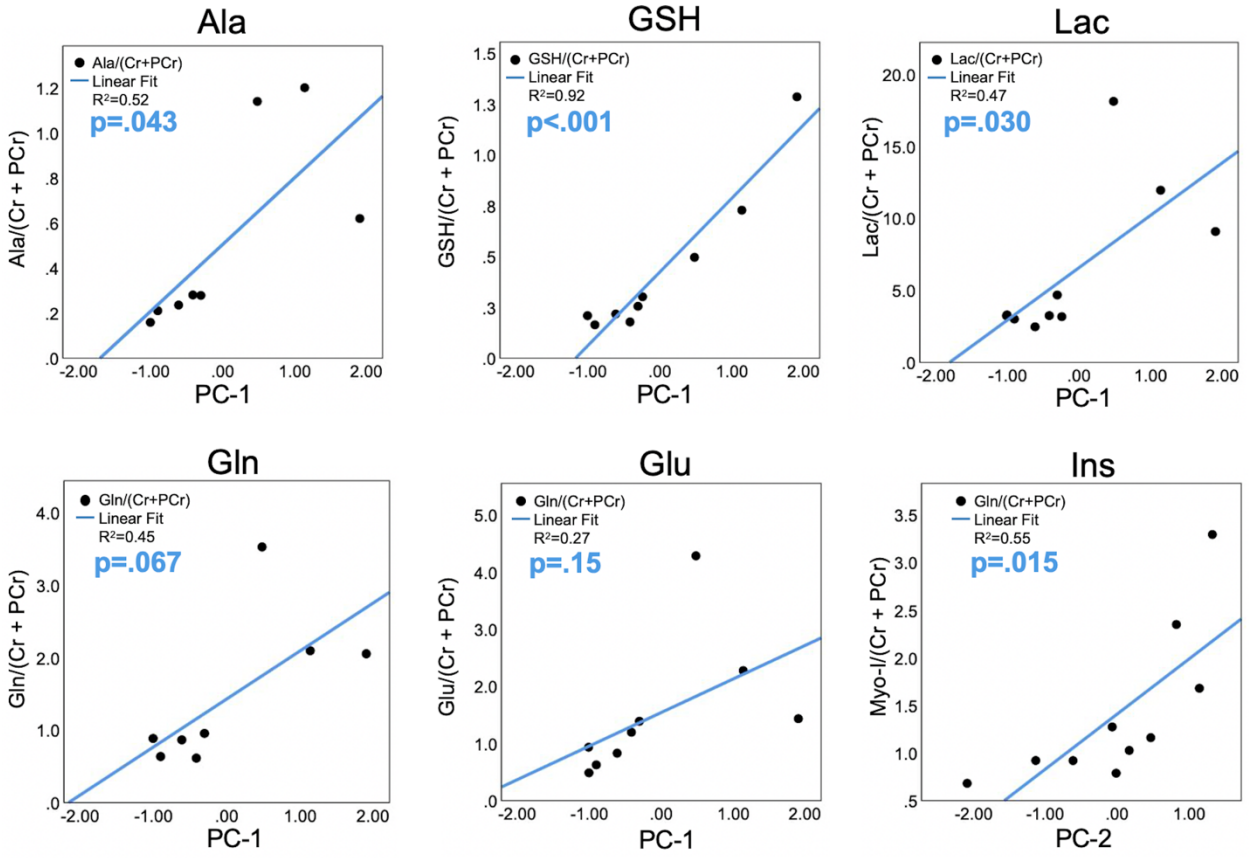

Figure 4. Significant associations between tumor metabolite concentrations and the principal components PC-1 contains contributions from IL-1A, IL-1B, IL-8, and CRP; PC-2 contains contributions from CRP

4. Discussion

In this study, ^{1}H HRMAS NMR was used to investigate glutamine as a potential imaging biomarker. Glutaminolysis is associated with glioma growth, and its role in tumor progression has been established.[7-11] The increase in concentrations of Gln, Glu, Ala, Lac, and GSH concentrations with grade seen in our data (Table 4, Table 5) support previous reports indicating that glutaminolysis is upregulated in higher grades of gliomas.[9, 16, 40] Glutaminolysis allows Gln and Glu to serve as precursors for Lac, Ala, and GSH, all metabolites that support mitochondrial respiration and cell growth.[7, 10] Lac provides NADPH for the production fatty acids, which are required for cell division and energy production.[41] In this process, Gln is converted to Ala which can be integrated into the TCA cycle and promote cell growth.[7, 9] GSH production has also been shown to be essential for glioma growth, and its production increases with grade.[11, 14] Furthermore, inhibition of enzymes involved in glutaminolysis have been shown to inhibit the transformation of glioma cells, suggesting that the increased reliance on glutaminolysis seen in gliomas is pivotal for its progression.[42, 43]

A number of studies indicate that chronic inflammation, which is present in most tumor microenvironments, is linked to cancer metabolic dysregulation.[21, 22] Inflammatory markers activate the transcription factors NF-kB and STAT3, which aggravate the Warburg effect and glutaminolysis by upregulating mitochondrial respiration as well as increasing glucose and glutamine uptake by cancer cells.[18, 44] The positive correlations between Gln, Ala, GSH, and Lac with the first inflammatory marker PC support these observations. PC-1 included contributions from inflammatory markers known to activate NF-kB and STAT-3.[18, 44-46] Inflammatory markers may play a role in the metabolic reprogramming to glutamine-based energetics through an NF-kB and STAT-3 dependent mechanism (Figure 5).

Metabolic reprogramming has come to be known as a hallmark of cancer, as it is present in many types of cancer cells.[6-8] As a result, pharmacologic strategies are increasingly targeting dysregulated metabolic pathways. Inhibition of enzymes involved in glutaminolysis and the Warburg effect are effective in slowing the growth of cancer cells, indicating a promising avenue for patients with tumors that exhibit metabolic reprogramming.[11, 15-17] Noninvasive identification of patients who may benefit from these treatments is paramount. The current diagnostic strategy of biopsy collection is limited, as the process is invasive and the biopsy samples provide pathological information without the context of metabolism.[3, 4] On the other hand, a combined MRI and MRS approach provides metabolic information that is not reflected in a biopsy alone.[47, 48] Methods employing MRI and MRS to quantify glutamine may indicate which patients might benefit from treatments targeting glutamine metabolism. Future work will expand on in vivo quantification of glutamine, as well as further characterizing the relationship between metabolism and the tumor microenvironment.

There were several limitations of this study. A small sample size was used, which reduced the statistical power of the results. ^{1}H HRMAS NMR analysis included 14 samples, and results must be validated with a larger sample. Notably, Cho and NAA did not change significantly with grade. As these metabolites commonly change with glioma grade, it may indicate a lack of statistical power.[27, 30, 49] Moreover, samples for ^{1}H HRMAS NMR was aliquoted using a 2 mm biopsy punch, which may not fully represent the molecular heterogeneity seen in whole tumors.

In this study, we present an approach to study the tumor microenvironment that utilizes ^{1}H HRMAS NMR and inflammatory markers quantification. Metabolites involved in glutaminolysis were positively associated with inflammation. Our findings identify glutamine as

a potential biomarker of metabolic reprogramming in gliomas. Future work will translate glutamine quantification to in vivo studies, which may aid in noninvasively diagnosing and monitoring treatment response in order to improve the prognosis of gliomas.

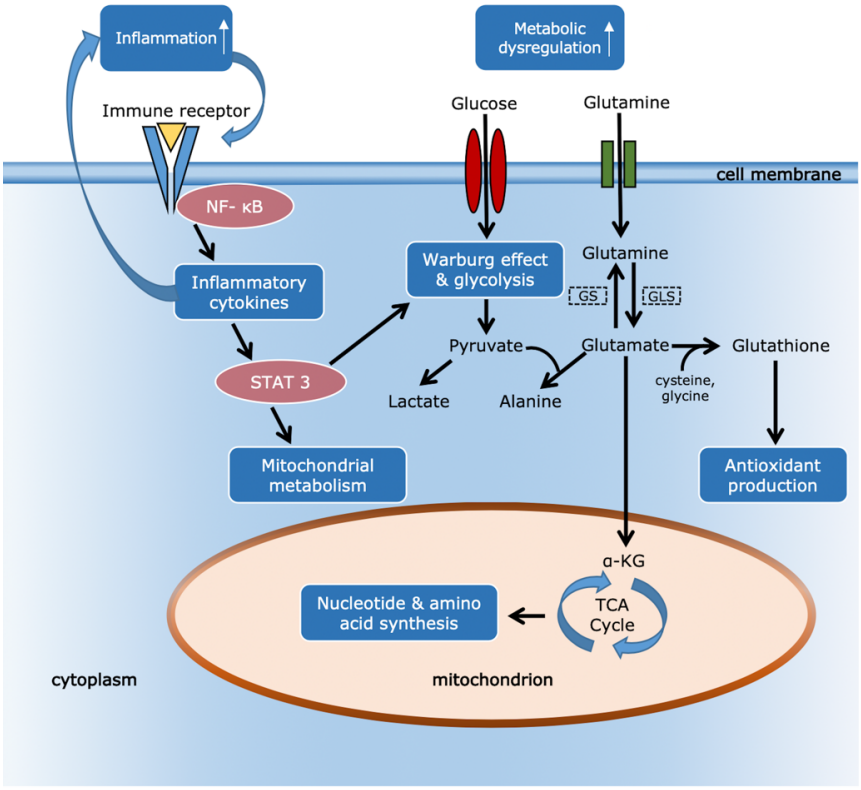

Figure 5. Schematic representing the relationship between inflammation and metabolic dysregulation in the tumor microenvironment GS=glutamine synthetase; GLS=glutaminase; TCA=tricarboxylic acid cycle; α-KG=α-ketoglutarate; NF-κB=nuclear factor kappa-light-chain-enhancer of activated B cells; STAT 3=signal transducer and activator of transcription 3

Note: Portions of this text and some of the figures and tables have been adapted, with permission, from References 33, 34, and 35. Adapted tables and figures are cited within the text.

References

1. Weller, M.; Wick, W.; Aldape, K.; Brada, M.; Berger, M.; Pfister, S. M.; Nishikawa, R.; Rosenthal, M.; Wen, P. Y.; Stupp, R.; Reifenberger, G., Glioma. *Nat Rev Dis Primers* **2015,** *1*, 15017.
2. Suzuki, H.; Aoki, K.; Chiba, K.; Sato, Y.; Shiozawa, Y.; Shiraishi, Y.; Shimamura, T.; Niida, A.; Motomura, K.; Ohka, F.; Yamamoto, T.; Tanahashi, K.; Ranjit, M.; Wakabayashi, T.; Yoshizato, T.; Kataoka, K.; Yoshida, K.; Nagata, Y.; Sato-Otsubo, A.; Tanaka, H.; Sanada, M.; Kondo, Y.; Nakamura, H.; Mizoguchi, M.; Abe, T.; Muragaki, Y.; Watanabe, R.; Ito, I.; Miyano, S.; Natsume, A.; Ogawa, S., Mutational landscape and clonal architecture in grade II and III gliomas. *Nat Genet* **2015,** *47* (5), 458-68.
3. Molinaro, A. M.; Taylor, J. W.; Wiencke, J. K.; Wrensch, M. R., Genetic and molecular epidemiology of adult diffuse glioma. *Nat Rev Neurol* **2019,** *15* (7), 405-417.
4. Cloughesy, T. F.; Cavenee, W. K.; Mischel, P. S., Glioblastoma: from molecular pathology to targeted treatment. *Annu Rev Pathol* **2014,** *9*, 1-25.
5. Wen, P. Y.; Kesari, S., Malignant gliomas in adults. *N Engl J Med* **2008,** *359* (5), 492-507.
6. Warburg, O.; Wind, F.; Negelein, E., The metabolism of tumors in the body. *J Gen Physiol* **1927,** *8* (6), 519-530.
7. Vander Heiden, M. G.; Cantley, L. C.; Thompson, C. B., Understanding the Warburg effect: the metabolic requirements of cell proliferation. *Science* **2009,** *324* (5930), 1029-1033.
8. Hanahan, D.; Weinberg, R. A., Hallmarks of cancer: the next generation. *Cell* **2011,** *144* (5), 646-74.
9. DeBerardinis, R. J.; Mancuso, A.; Daikhin, E.; Nissim, I.; Yudkoff, M.; Wehrli, S.; Thompson, C. B., Beyond aerobic glycolysis: transformed cells can engage in glutamine metabolism that exceeds the requirement for protein and nucleotide synthesis. *Proc Natl Acad Sci U S A* **2007,** *104* (49), 19345-19350.
10. Ward, P. S.; Thompson, C. B., Metabolic reprogramming: a cancer hallmark even Warburg did not anticipate. *Cancer Cell* **2012,** *21* (3), 297-308.
11. Choi, Y. K.; Park, K. G., Targeting glutamine metabolism for cancer treatment. *Biomol Ther (Seoul)* **2018,** *26* (1), 19-28.
12. Westergaard, N.; Sonnewald, U.; Schousboe, A., Metabolic trafficking between neurons and astrocytes: the glutamate/glutamine cycle revisited. *Dev Neurosci* **1995,** *17* (4), 203-211.
13. Albrecht, J.; Sidoryk-Wegrzynowicz, M.; Zielinska, M.; Aschner, M., Roles of glutamine in neurotransmission. *Neuron Glia Biol* **2010,** *6* (4), 263-276.
14. Altman, B. J.; Stine, Z. E.; Dang, C. V., From Krebs to clinic: glutamine metabolism to cancer therapy. *Nat Rev Cancer* **2016,** *16* (10), 619-634.
15. Plaitakis, A.; Kalef-Ezra, E.; Kotzamani, D.; Zaganas, I.; Spanaki, C., The glutamate dehydrogenase pathway and its roles in cell and tissue biology in health and disease. *Biology (Basel)* **2017,** *6* (1), 11.
16. Phan, L. M.; Yeung, S. C.; Lee, M. H., Cancer metabolic reprogramming: importance, main features, and potentials for precise targeted anti-cancer therapies. *Cancer Biol Med* **2014,** *11* (1), 1-19.
17. Tanaka, K.; Sasayama, T.; Irino, Y.; Takata, K.; Nagashima, H.; Satoh, N.; Kyotani,

K.; Mizowaki, T.; Imahori, T.; Ejima, Y.; Masui, K.; Gini, B.; Yang, H.; Hosoda, K.; Sasaki, R.; Mischel, P. S.; Kohmura, E., Compensatory glutamine metabolism promotes glioblastoma resistance to mTOR inhibitor treatment. *J Clin Invest* **2015,** *125* (4), 1591-1602.

18. Xia, Y.; Shen, S.; Verma, I. M., NF-kappaB, an active player in human cancers. *Cancer Immunol Res* **2014,** *2* (9), 823-30.
19. DeNardo, D. G.; Andreu, P.; Coussens, L. M., Interactions between lymphocytes and myeloid cells regulate pro- versus anti-tumor immunity. *Cancer Metastasis Rev* **2010,** *29* (2), 309-316.
20. Mantovani, A.; Allavena, P.; Sica, A.; Balkwill, F., Cancer-related inflammation. *Nature* **2008,** *454* (7203), 436-44.
21. Biswas, S. K., Metabolic reprogramming of immune cells in cancer progression. *Immunity* **2015,** *43* (3), 435-449.
22. Haroon, E.; Woolwine, B. J.; Chen, X.; Pace, T. W.; Parekh, S.; Spivey, J. R.; Hu, X. P.; Miller, A. H., IFN-alpha-induced cortical and subcortical glutamate changes assessed by magnetic resonance spectroscopy. *Neuropsychopharmacology* **2014,** *39* (7), 1777-1785.
23. Afrasiabi, K.; Zhou, Y.-H.; Fleischman, A., Chronic inflammation: is it the driver or is it paving the road for malignant transformation? *Genes Cancer* **2015,** *6* (5-6), 214-219.
24. Palsson-McDermott, E. M.; O'Neill, L. A., The Warburg effect then and now: from cancer to inflammatory diseases. *Bioessays* **2013,** *35* (11), 965-973.
25. Cheng, L. L.; Ma, M. J.; Becerra, L.; Ptak, T.; Tracey, I.; Lackner, A.; González, R. G., Quantitative neuropathology by high resolution magic angle spinning proton magnetic resonance spectroscopy. *Proc Natl Acad of Sci USA* **1997,** *94* (12), 6408-6413.
26. Ross, B. D., Biochemical considerations in 1H spectroscopy. Glutamate and glutamine; myo-inositol and related metabolites. *NMR Biomed* **1991,** *4* (2), 59-63.
27. Pandey, R.; Caflisch, L.; Lodi, A.; Brenner, A. J.; Tiziani, S., Metabolomic signature of brain cancer. *Mol Carcinog* **2017,** *56* (11), 2355-2371.
28. Bogner, W.; Hangel, G.; Esmaeili, M.; Andronesi, O. C., 1D-spectral editing and 2D multispectral in vivo 1H-MRS and 1H-MRSI - methods and applications. *Anal Biochem* **2017,** *529*, 48-64.
29. Cheng, L. L.; Chang, I. W.; Louis, D. N.; Gonzalez, R. G., Correlation of high-resolution magic angle spinning proton magnetic resonance spectroscopy with histopathology of intact human brain tumor specimens. *Cancer Res* **1998,** *58* (9), 1825-1832.
30. Horska, A.; Barker, P. B., Imaging of brain tumors: MR spectroscopy and metabolic imaging. *Neuroimaging Clin N Am* **2010,** *20* (3), 293-310.
31. Hyare, H.; Thust, S.; Rees, J., Advanced MRI techniques in the monitoring of treatment of gliomas. *Curr Treat Options Neurol* **2017,** *19* (3), 11.
32. Liu, J.; Li, C.; Chen, Y.; Lv, X.; Lv, Y.; Zhou, J.; Xi, S.; Dou, W.; Qian, L.; Zheng, H.; Wu, Y.; Chen, Z., Diagnostic performance of multiparametric MRI in the evaluation of treatment response in glioma patients at 3T. *J Magn Reson Imaging* **2019**, *51*(4), 1154-1161.
33. Ekici, S.; Geryak, R.; Fleischer, C. C. Comparison of LCModel fitting of HRMAS spectra acquired from malignant glioma tissue using free induction decay and Carr-Purcell-Meiboom-Gill pulse sequences, *Proc Intl Soc Mag Reson Med* **2019** (27), 2281.

34. Ekici S.; Geryak, R.; Neill, S.G.; Shu, H.K.; Fleischer, C.C. Improved fitting of HRMAS NMR spectra for ex vivo metabolomic analysis of glioma tissue, *Cancer Res* July 1 **2019** *79* (13 Supplement), 3721.
35. Ekici, S.; Fleischer, C. C. Association of tumor metabolites with inflammation in the glioma microenvironment studied with HRMAS NMR, *Proc Intl Soc Mag Reson Med* **2020** (28), 1452.
36. Provencher, S., Estimation of metabolite concentrations from localized in vivo proton NMR spectra. *Magn Reson Med.* **1993,** *30* (6), 672-679.
37. Schulte, R. F.; Lange, T.; Beck, J.; Meier, D.; Boesiger, P., Improved two-dimensional J-resolved spectroscopy. *NMR Biomed* **2006,** *19* (2), 264-270.
38. Jolliffee, I.T.; Cadima, J., Principal component analysis: a review and recent developments. *Philos Trans A Math Phys Eng Sci* **2016,** *374* (2065), 20150202.
39. Tabachnick, B. G.; Fidell, L. S., *Using multivariate statistics*. 5 ed.; Allyn & Bacon/Pearson Education: Boston, MA, 2007; p 644-646.
40. Bi, J.; Chowdhry, S.; Wu, S.; Zhang, W.; Masui, K.; Mischel, P. S., Altered cellular metabolism in gliomas - an emerging landscape of actionable co-dependency targets. *Nat Rev Cancer* **2020,** *20* (1), 57-70.
41. Lin, H.; Patel, S.; Affleck, V. S.; Wilson, I.; Turnbull, D. M.; Joshi, A. R.; Maxwell, R.; Stoll, E. A., Fatty acid oxidation is required for the respiration and proliferation of malignant glioma cells. *Neuro-oncology* **2017,** *19* (1), 43-54.
42. Wang, J. B.; Erickson, J. W.; Fuji, R.; Ramachandran, S.; Gao, P.; Dinavahi, R.; Wilson, K. F.; Ambrosio, A. L.; Dias, S. M.; Dang, C. V.; Cerione, R. A., Targeting mitochondrial glutaminase activity inhibits oncogenic transformation. *Cancer Cell* **2010,** *18* (3), 207-219.
43. Yang, C.; Sudderth, J.; Dang, T.; Bachoo, R. M.; McDonald, J. G.; DeBerardinis, R. J., Glioblastoma cells require glutamate dehydrogenase to survive impairments of glucose metabolism or Akt signaling. *Cancer Res* **2009,** *69* (20), 7986-7993.
44. Mauro, C.; Leow, S. C.; Anso, E.; Rocha, S.; Thotakura, A. K.; Tornatore, L.; Moretti, M.; De Smaele, E.; Beg, A. A.; Tergaonkar, V.; Chandel, N. S.; Franzoso, G., NF-kappaB controls energy homeostasis and metabolic adaptation by upregulating mitochondrial respiration. *Nat Cell Biol* **2011,** *13* (10), 1272-1279.
45. Landskron, G.; De la Fuente, M.; Thuwajit, P.; Thuwajit, C.; Hermoso, M. A., Chronic inflammation and cytokines in the tumor microenvironment. *J Immunol Res* **2014,** *2014*, 149185.
46. Shrotriya, S.; Walsh, D.; Bennani-Baiti, N.; Thomas, S.; Lorton, C., C-reactive protein is an important biomarker for prognosis tumor recurrence and treatment response in adult solid tumors: a systematic review. *PloS One* **2015,** *10* (12), 143080.
47. Coquery, N.; Stupar, V.; Farion, R.; Maunoir-Regimbal, S.; Barbier, E. L.; Rémy, C.; Fauvelle, F., The three glioma rat models C6, F98 and RG2 exhibit different metabolic profiles: in vivo 1H MRS and ex vivo 1H HRMAS combined with multivariate statistics. *Metabolomics* **2015,** *11* (6), 1834-1847.
48. Cheng, L. L.; Anthony, D. C.; Comite, A. R.; Black, P. M.; Tzika, A. A.; Gonzalez, R. G., Quantification of microheterogeneity in glioblastoma multiforme with ex vivo high-resolution magic-angle spinning (HRMAS) proton magnetic resonance spectroscopy. *Neuro Oncol* **2000,** *2* (2), 87-95.
49. Oz, G.; Alger, J. R.; Barker, P. B.; Bartha, R.; Bizzi, A.; Boesch, C.; Bolan, P. J.;

Brindle, K. M.; Cudalbu, C.; Dinçer, A.; Dydak, U.; Emir, U. E.; Frahm, J.; González, R. G.; Gruber, S.; Gruetter, R.; Gupta, R. K.; Heerschap, A.; Henning, A.; Hetherington, H. P.; Howe, F. A.; Hüppi, P. S.; Hurd, R. E.; Kantarci, K.; Klomp, D. W. J.; Kreis, R.; Kruiskamp, M. J.; Leach, M. O.; Lin, A. P.; Luijten, P. R.; Marjańska, M.; Maudsley, A. A.; Meyerhoff, D. J.; Mountford, C. E.; Nelson, S. J.; Pamir, M. N.; Pan, J. W.; Peet, A. C.; Poptani, H.; Posse, S.; Pouwels, P. J. W.; Ratai, E.-M.; Ross, B. D.; Scheenen, T. W.; Schuster, C.; Smith, I. C. P.; Soher, B. J.; Tkáč, I.; Vigneron, D. B.; Kauppinen, R. A.; Group, M. R. S. C., Clinical proton MR spectroscopy in central nervous system disorders. *Radiology* **2014,** *270* (3), 658-679.